

International Journal of Automation and Control

ISSN online: 1740-7524 - ISSN print: 1740-7516

https://www.inderscience.com/ijaac

Design of a model predictive-based fault estimator for faulty nonlinear switched dynamics with guaranteed recursive feasibility

Li Wang

DOI: 10.1504/IJAAC.2025.10074193

Article History:

Received: 30 April 2025
Last revised: 18 August 2025
Accepted: 20 August 2025
Published online: 24 October 2025

Design of a model predictive-based fault estimator for faulty nonlinear switched dynamics with guaranteed recursive feasibility

Li Wang

School of Mechanical Engineering, Chongqing Industry Polytechnic University, Chongqing, 400020, China Email: cqipcwangly@163.com

Abstract: This research presents a defect estimation framework employing a model predictive approach for switched nonlinear systems. The method integrates system states and failure signals into an augmented state-space model. The squared Euclidean norm of the estimation error over the prediction horizon serves as the performance metric, minimised through a set of linear matrix inequality constraints to ensure asymptotic stability. The estimator design enforces constrained estimation error to remain within a defined threshold, enhancing robustness. Recursive feasibility is analytically demonstrated at each time step. The approach is validated on a continuous stirred tank reactor, a key component in the petrochemical industry. In fault-free conditions, with estimation error maintained below 0.05. The estimator effectively detects and quantifies both constant and time-varying faults. The system's energy function consistently decreases, confirming the asymptotic stability of the estimation error dynamics and supporting its application in fault-tolerant control.

Keywords: fault estimation; switched nonlinear systems; model predictive control; augmented state-space model; linear matrix inequality; recursive feasibility; asymptotic stability; continuous stirred tank reactor.

Reference to this paper should be made as follows: Wang, L. (2025) 'Design of a model predictive-based fault estimator for faulty nonlinear switched dynamics with guaranteed recursive feasibility', *Int. J. Automation and Control*, Vol. 19, No. 7, pp.1–22.

Biographical notes: Li Wang works at the Chongqing Industry Polytechnic College's School of Mechanical Engineering in China. He works as a Faculty Member focuses on applied research, mechanical engineering education, and incorporating cutting-edge technology into technical and vocational training. With an emphasis on improving the development of practical skills and industry-academia collaboration, his professional knowledge encompasses mechanical design, manufacturing processes, and engineering applications. Additionally, he actively participates in applied research initiatives that promote workforce development and industrial growth in the region.

1 Introduction

In the past, various methods for modelling physical systems have been presented. Despite considering uncertainty terms in these methods, they are not able to describe the behaviour of the system in different situations. Therefore, it is better to extract a dynamic model compatible with each situation, and then by connecting these dynamic models, a comprehensive model is formed. This comprehensive model displays a switched system, and different situations represent the switching law Nodozi et al. (2017). Based on the concept of switching, many physical systems that have complex behaviour or are under faults and structural shifts can be represented by switched systems. Therefore, engineers in the field of control pay special attention to this type of modelling and try to develop the regulator and observer based on the concept of switching to increase the probability of the desired performance of the regulator and observer in real industrial conditions. Unlike non-switched systems, checking stability in switched systems is influenced by the specification of the switching signal. Before design, the frequency of the switching law can be considered unlimited or limited. The assumption that the frequency of the switching law is unlimited is too strict and not compatible with real-world conditions. One of the common methods for limiting the frequency is the time-dependent method, which establishes a time compromise between the duration of each dynamic.

The time-dependent method is classified into different structures, which can be referred to as average dwell time (ADT) and persistent dwell time (PDT) (Shi et al., 2019; Zheng et al., 2018). A key issue in practical systems is the issue of faults. The occurrence of a fault endangers the reliability of the system and can lead to system instability and serious damage to it. Therefore, a platform must be provided to calculate the time of fault occurrence and its exact amount at every moment so that the necessary measures can be taken to deal with it. A common solution for fault detection and estimation is the design of a state observer or fault estimator, which has been of interest since the past. In switching systems, this issue becomes more complicated because the switching signal has a great influence on the dynamic stability of the formed prediction error. Based on the Luenberger structure, Lyu et al. (2020) and Zheng et al. (2020) extended ADT-based Luenberger observers through multiple Lyapunov functions (MLF) for linear and nonlinear switched dynamics. Among the most important weaknesses of these research, we can mention the ignoring of the fault, the ignoring of the efficiency metric, and their resistance against a small class of switching rules. According to an adaptive concept, researchers in Li et al. (2017), Li and Tong (2017) and Liu et al. (2020) recommended ADT-based adaptive observers for strict and non-strict feedback dynamics.

In this research, observers are created for a certain class of systems without considering faults, and they are not effective for the current research system. Based on unknown input structure, Chen et al. (2019) and Du et al. (2019) introduced ADT-based unknown input observers (UIOs) through MLF to eliminate the unknown input effects. Based on model predictive structure, Qi et al. (2021), Taghieh et al. (2021) and Zhang et al. (2024) recommended ADT and PDT-based model predictive observers through MLF for Lipschitz switched dynamics. In these studies, the issue of reducing an efficiency metric is raised, but no attempt is made to estimate the fault. The conducted research confirms that only in Zhang et al. (2024), the development of the observer through the model predictive approach to minimise the efficiency metric has been discussed. Since there is a possibility of failure in practical systems, the designed observers will not be able to estimate the system states, and the estimation accuracy will

decrease. Also, fault detection and estimation are the main steps for designing a fault-tolerant regulator to increase reliability. Hence, this paper develops a fault estimator based on a model prediction approach for switched nonlinear dynamics. In this regard, system states and faults are considered as states of an augmented system.

Then, the L2 norm of the estimation error signals over the predictive horizon is regarded as the efficiency metric, and further, with the help of the model predictive concept and the stability criterion over the predictive horizon, the issue of reducing the efficiency metric becomes the problem of reducing the ceiling of the efficiency metric. On the other hand, the stability criterion is added to the enhancement issue as a linear matrix inequality constraint to form an L2 problem with an asymptotic stability guarantee. Also, the assumption of estimation error saturation is considered an important concern for having a specific error bound. In addition, the challenge of the recursive feasibility of the issue is analysed, and its answer is proved in each time step. The key ideas of this paper are outlined below:

- development of a fault estimator with the help of creating augmented states and the model predictive concept for Lipshitz switched dynamics
- solving an L2 problem along with an asymptotic stability guarantee for estimation error dynamics through the model predictive concept
- analysing the recursive feasibility to guarantee having an answer at each time step.

2 Literature review

Schwenzer et al. (2021) examined model-based predictive control (MPC) as a sophisticated method that employs process models to derive control actions via optimisation. They highlighted that MPC facilitated the management of intricate systems beyond the reach of conventional controllers, and that its model-centric architecture streamlined tuning and enhanced system comprehension. Their review encompassed recent theoretical advancements, practical implementations, and ways to tackle computing problems, thereby addressing a deficiency in the current literature on contemporary MPC progressions. Wang et al. (2024) introduced Memory Mamba, a memory-augmented state space model, to overcome the shortcomings of traditional defect detection techniques in managing complicated and imbalanced data. Through the integration of memory mechanisms, the model proficiently incorporated defect-specific characteristics and long-range interdependence. Memory Mamba was assessed using four industrial datasets and consistently surpassed existing methods, exhibiting remarkable adaptability and precision in various defect recognition tasks. Zuo et al. (2022) introduced SPADE, a hybrid model that integrates state space models with local attention to address the inefficiencies of Transformers in processing lengthy sequences.

SPADE employs a state space layer to encapsulate global dependencies while utilising local attention in upper layers for enhanced efficiency. Experiments conducted on the Long-Range Arena and language challenges demonstrated SPADE's exceptional performance and scalability in both comprehension and generation tasks. Duník et al.

(2024) suggested a methodology for detecting state noise in data-augmented physics-based models of nonlinear stochastic systems. They enhanced the precision and reliability of state estimation through maximum likelihood and correlation-based methodologies. Simulations in a tracking context revealed the efficacy of the method in improving data-driven dynamic models. Geromel (2023) analysed the characteristics of discrete-time linear matrix inequalities (DLMIs) and proposed a comprehensive numerical approach for their resolution. He illustrated the method's practicality and efficiency through several instances, emphasising that, due to the non-uniqueness of DLMI solutions, the goal was to identify any feasible solution that met the boundary criteria. Zhang et al. (2024) suggested a Lyapunov-based model predictive control approach employing deep learning to stabilise continuous-time nonlinear systems. They utilised neural ordinary differential equations to model system dynamics and created a deep neural network-based Lyapunov function that does not rely on affine assumptions.

The method, incorporated within a predictive control framework with tube-based safety limitations, guaranteed stability and safety. Simulations of a chemical process confirmed its efficacy. Liu et al. (2024) proposed a model predictive control methodology for limited output regulation in discrete-time linear systems. They tackled stability and feasibility concerns related to external signal estimates by reformulating the system and devising robust invariant sets. A hierarchical control mechanism guaranteed constraint compliance, and simulations validated the method's efficacy, even with incomplete signal data. Granzotto et al. (2024) investigated policy iteration for nonlinear discrete-time systems with non-discounted costs. They formulated criteria for recursive robust stability and bounded suboptimality under the premise that policy iteration remained recursively viable. After demonstrating that feasibility might fail in specific instances, they introduced a revised algorithm, PI+, which guaranteed recursive feasibility while maintaining both stability and near-optimality under modest assumptions. Abbasi and Huang (2024) suggested a fault diagnosis and tolerant control methodology for nonlinear industrial systems characterised by various operating areas. They minimised online computation by integrating fuzzy-based realisation with a subspace-aided method, utilising offline parity vector creation.

The technology, when applied to a continuous stirred tank reactor, attained elevated diagnostic accuracy and facilitated fault-tolerant, stable operation under diverse settings. Sarbaz (2024) tackled time-varying delays in state and input vectors by presenting a model predictive control method grounded in the Razumikhin approach. The interval type-2 fuzzy Takagi-Sugeno model enhanced delay management and system stability while decreasing complexity using linear matrix inequalities. An illustration showcased its efficacy and computational efficiency.

2.1 Research gaps and novelties

Despite the development of numerous fault diagnosis and observer design methodologies for nonlinear and switching systems, some significant issues persist unresolved. Current methodologies such as Luenberger observers, UIOs, and adaptive observers generally fail to precisely estimate fault signals, especially in dynamic switching scenarios. Numerous solutions either disregard fault modelling entirely or are restricted by assumptions

regarding system architecture or confined switching protocols. Moreover, current works on model predictive control in observer design have predominantly concentrated on minimising performance measures, neglecting the integration of fault estimating, error bounds, or stability within practical limits. A significant constraint in many of these methodologies is the lack of assurance for recursive feasibility, which is vital for maintaining ongoing functionality in real-time industrial systems. This paper presents a unique fault estimation approach utilising model predictive control specifically designed for switched nonlinear systems to address these deficiencies. The method dramatically enhances the state-space model to concurrently estimate both system states and failure signals. The performance measure is defined as the squared Euclidean norm of the estimate error across the prediction horizon, utilising a linear matrix inequality formulation to ensure asymptotic stability.

This work's principal novelty is the integration of estimating error saturation and a thorough examination of recursive feasibility, guaranteeing constrained error behaviour and dependable online performance. The efficacy of the suggested method is illustrated via simulation on a continuous stirred tank reactor system, underscoring its applicability in safety-critical and fault-sensitive industrial settings.

2.2 Paper organisation

The subsequent sections of this work are organised as follows: Section 2 delineates the numerical execution of the proposed fault estimation framework applied to a continuous stirred tank reactor system; a benchmark model emblematic of actual industrial processes. Two simulation scenarios are examined: one under nominal (fault-free) conditions and another with actuator malfunctions. These case studies are employed to assess the precision, resilience, and real-time application of the suggested estimator. Section 3 presents a comprehensive examination of the simulation results, incorporating a comparative evaluation with current fault estimation methodologies. The discourse examines the estimator's practical significance, underscores its existing limitations, and delineates potential directions for further inquiry. Section 4 closes the work by reviewing the principal contributions and delineating avenues for further research and experimental validation.

3 Main outcomes

Imagine the adaptive approach of the system is explained by the subsequent equations.

$$x(k+1) = G_{s(k)}x(k) + H_{s(k)}h(k) + \eta_{s(k)}(x(k)) + J_{s(k)}e(k) \quad y(k) = Cx(k)$$
(1)

 $x(k) \in n^{\eta x}$, $h(k) \in n^{nh}$, $e(k) \in n^{ne}$, and $y(k) \in n^{ny}$ denote the states, inputs, faults, and outputs, respectively. The switching signal is represented by s(k). The state-space matrices are denoted by $G_{s(k)}$, $H_{s(k)}$, C, and $J_{s(k)}$, while $\eta_{\sigma(k)}(x(k))$ displays the nonlinear term. The faults are assumed to be time-varying. Accordingly, this work supposes that the second difference of e(k) concerning the step is zero. To estimate faults, the system's state variables are augmented as follows:

$$S(k+1) = \overline{G}_{s(k)}S(k) + \overline{H}_{s(k)}h(k) + \overline{\eta}_{s(k)}(S(k)) \quad y(k) = \overline{C}S(k)$$
 (2)

When considering the augmented states mentioned above, the dynamic model expressed in equation (1) undergoes modifications as follows:

$$S(k+1) = \overline{G}_{s(k)}S(k) + \overline{H}_{s(k)}h(k) + \overline{\eta}_{s(k)}(S(k)) \quad y(k) = \overline{C}S(k)$$
(3)

where

$$\vec{G}_{s(k)} = \begin{pmatrix} \vec{G}_{s(k)} & J_{s(k)} & 0 \\ 0 & 0 & I \\ 0 & -I & 2I \end{pmatrix}, \vec{H}_{s(k)} = \begin{pmatrix} H_{s(k)} \\ 0 \\ 0 \end{pmatrix}, \eta_{s(k)} \left(S(k) \right) = \begin{pmatrix} \eta_{s(k)} \left(x(k) \right) \\ 0 \\ 0 \end{pmatrix},
\vec{C} = \begin{pmatrix} C & 0 & 0 \end{pmatrix} \tag{4}$$

To design a fault estimator, the following initial actions are necessary:

Lemma 1 (Petersen, 1987): The relationship between matrices V and W and scalars a > 0, can be expressed as follows:

$$V^T W + W^T V \le a V^T V + a^{-1} W^T W \tag{5}$$

Definition 1 (Zhang et al., 2015): The defined interval is split into multiple windows utilising the PDT approach. Each window encompasses two parts: the m-part and the T-part. Within the m-part, a specific subsystem is executed. In the m-part, a particular sub-system is operated for a minimum duration of k_m . In the T-part, the switches happen at a rate lower than ω and with an operation duration less than k_T . The overall count of switches in the m-part of each window is restricted to $n(k_{S_q+1}, k_{S_{q+1}}) \le k_T \omega$.

A potential solution for a Luenberger observer is presented below:

$$\hat{S}(k+1) = \bar{G}_{s(k)} \hat{S}(k) + \bar{H}_{s(k)} h(k) + \bar{\eta}_{\sigma(k)} (\hat{S}(k)) + F_{s(k),k} (y(k) - y(k))$$
(6)

The state estimation, displayed as S, and the output estimation, represented as \hat{y} , are utilised in conjunction with the estimator gain $H_{\sigma(k),k}$. The state estimation error can be computed as:

$$d(k+1) = S(k+1) - \hat{S}(k+1) = (\overline{G}_{s(k)}S(k) + \overline{H}_{s(k)}h(k) + \overline{\eta}_{s(k)}(S(k)))$$

$$- (\overline{G}_{s(k)}\hat{S}(k) + \overline{H}_{s(k)}h(k) + \eta_{s(k)}(\hat{S}(k))$$

$$+ F_{s(k),k}(y(k) - \hat{y}(k))) = \overline{G}_{s(k)}(S(k) - \hat{S}(k))$$

$$+ (\overline{\eta}_{s(k)}(S(k)) - \eta_{\sigma(k)}(\hat{S}(k))) + F_{s(k),k}C(S(k) - \hat{S}(k)))$$

$$= (G_{s(k)} - F_{s(k),k}C)d(k) + \tilde{\eta}_{s(k)}$$

$$(7)$$

In this scenario, the model predictive approach is stated, and the expression of the state estimation error across the projection period is detailed as:

$$d(k+r+1|k) = (G_{s(k)} - F_{s(k),k}(k+r|k)C)d(k+j|k) + \tilde{\eta}_{s(k)}, r = 0,1,...,\infty$$
 (8)

In equation (8), the variable d(k + r|k) displays the predicted state estimation error in j steps ahead. It is assumed that the predicted state estimation error is constrained according to the following limits:

$$|d_m(k+r|k)| \le d_{m \max}, \ m=1,...,n_d, \ r=0,1,...,\infty$$
 (9)

where d_m is the mth component of d.

The objective function is defined as follows:

$$J_{s(k),k} = \sum_{r=0}^{\infty} d(k+r|k)^{T} d(k+r|k)$$
(10)

The Lyapunov stability conditions is considered:

$$I_{s(k+r+1|k),k}(k+r+1|k) - I_{s(k+r|k),k}(k+r|k) \le \tau_s I_{s(k+r|k),k}(k+r|k) -d(k+r|k)^T d(k+r|k), r = 0,1,...,\infty$$
(11)

$$\forall i, l \in s(k), i \neq l : I_i(e(k_s)) \le fI_i(e(k_s)), i = s(k_s), l = s(k_s - 1)$$
(12)

In the aforementioned equation, k_S displays the switching time step, f denotes the energy variation constant at time k_S , and I corresponds to the energy function. Ultimately, the model predictive estimator (MPE) can be expressed as:

The objective is to determine an estimator gain at any stage that satisfies the conditions specified in equations (11), (12), and the constraint presented in equation (9), and minimises the objective function defined in equation (10). Taking into account the s(k+r+1|k) = s(k+r|k) = s(k) = i, t=k+r|k, and t+1=k+r+1|k, the problem of the framework estimator can be formulated in the following manner:

$$\min \max J_{i,k} \text{ subject to: } I_{i,k}(t+1) - I_{i,k}(t) \le \tau_s I_{i,k}(t) - d(t)^T d(t)$$

$$\forall i, l \in s(k), i \ne l : I_i(e(k_s)) \le f I_l(e(k_s)), i = s(k_s), l = s(k_s-1) |d_m(t)| \le de_{m,max}$$

$$(13)$$

If it regards the maximum of the objective metric as $\rho_{i,k}$, the formulation of the MPE issue is:

$$\min \rho_{i,k} \text{ subject to: } I_{i,k}(t+1) - I_{i,k}(t) \le \tau_s I_{i,k}(t) - d(t)^T d(t)$$

$$\forall i, l \in s(k), i \ne l : I_i(d(k_s)) \le f I_l(d(k_s)), i = s(k_s), l = s(k_s - 1) \ J_{s(k),k} \le \rho_{i,k}$$

$$|d_m(t)| \le dd_{m,max}$$
(14)

Theorem 1: Suppose the state estimation error dynamics are given by equation (7). Let $\tau_S < 0$, f > 1, and $a_i > 0$ be known, and k_T and ω be specified for the PDT concept requirements If there exist $n_{i,k} > 0$, $O_{i,k}$, and $\Psi_{i,k} > 0$, enabling the following problem to have a solution:

$$subject \ to: \\ \begin{pmatrix} (1+\tau_{s})V_{i,k} & \sqrt{1+a_{i}^{-1}}\vartheta_{i}V_{i,k}^{T}T_{i} & V_{i,k}^{T} & \sqrt{1+a_{i}}(V_{i,k}^{T}\overline{G}_{i}^{T}-O_{i,k}^{T}) \\ * & \Psi_{i,k}I & 0 & 0 \\ * & * & I & 0 \\ * & * & * & V_{i,k} \end{pmatrix} \geq 0 \\ V_{i,k} - \Psi_{i,k}I \geq 0 \\ \begin{pmatrix} V_{i,k} - f^{-1}V_{l,k-1} \geq 0 \\ 0 & -V_{i,k} \end{pmatrix} \leq 0 \\ \begin{pmatrix} e_{m,\max} & V_{i,k} \\ * & V_{i,k} \end{pmatrix} \geq 0, \ m = 1,...,n_{d} \end{pmatrix}$$

$$(15)$$

where V^m is defined as $V^m = (0,...,0, 1,0,...,0,...,0)$, then for a switched estimator in equation (6) with $F_{i,k} = O_{i,k} T_{i,k}^{-1} C^{\dagger}$ and any PDT structure with the following range:

$$k_m > k_m^* = \max(\frac{(k_T \omega + 1)\ln f}{-\ln(1 + \tau_s)}, \frac{1}{\omega})$$
(16)

the state estimation error dynamic in equation (7) is an asymptotical stable.

Proof. Assume the energy function according to the following equation:

$$I_{i,k}(d(t)) = d(t)^T \Pi_{i,k} d(t), \Pi_{i,k} > 0$$
(17)

The first condition in equation (14) is expanded according to following equation:

$$I_{i,k}(d(t+1)) - I_{i,k}(d(t)) = d^{T}(t+1)\Pi_{i,k}d(t+1) - d^{T}(t)\Pi_{i,k}d(t) = ((\overline{G}_{i} - \overline{F}_{i,k}C))$$

$$d(T) + \tilde{\eta}_{i})^{T}\Pi_{i,k}((\overline{G}_{i} - \overline{F}_{i,k}C)d(t) + \tilde{\eta}_{i}) - d(t)^{T}\Pi_{i,k}d(t)$$
(18)

Using Lemma 1, it gets:

$$I_{i,k}(d(t+1)) - I_{i,k}(d(t)) \le (1+a_i)d(t)^T (\bar{G}_i - \bar{F}_{i,k}C)^T \Pi_{i,k} (\bar{G}_i - \bar{F}_{i,k}C)d(t)$$

$$+ (1+a_i^{-1})\tilde{\eta}_i^T \Pi_{i,k}\tilde{\eta}_i - d(t)^T \Pi_{i,k}d(t)$$
(19)

Considering:

$$\Pi_{ik} \le \theta_{ik} I \tag{20}$$

Consider the following condition over the nonlinear term:

$$\| \, \overline{\eta}_{s(k)}(S(k)) - \overline{\eta}_{s(k)}(\hat{S}(k)) \| \le \overline{\beta}_{s(k)} \| \, \overline{T}_{s(k)}(S(k) - \hat{S}(k)) \| \tag{21}$$

It obtains:

$$I_{i,k}(d(t+1)) - I_{i,k}(d(t)) \le (1+a_i)d(t)^T (\overline{G}_i - \overline{F}_{i,k}C)^T \Pi_{i,k} (\overline{G}_i - \overline{F}_{i,k}C)d(t)$$

$$+ (1+a_i^{-1})\theta_{i,k}\overline{\beta}_i^2 d(t)^T T_i^T \overline{T}_i d(t) - d(t)^T \Pi_{i,k} d(t)$$
(22)

Substituting equation (22) into the first condition of the enhancement issue in equation (14), it will have:

$$(1+a_{i})d(t)^{T}(\bar{G}_{i}-\bar{F}_{i,k}C)^{T}\Pi_{i,k}(\bar{G}_{i}-\bar{F}_{i,k}C)d(t)+(1+a_{i}^{-1})$$

$$\theta_{i,k}\bar{\beta}_{i}^{2}d(t)^{T}\bar{T}_{i}^{T}\bar{T}_{i}d(t)-d(t)^{T}\Pi_{i,k}d(t)-\tau_{s}d(t)^{T}\Pi_{i,k}d(t)+d(t)^{T}d(t)\leq0$$
(23)

Equation (23) is expanded according to the subsequent equation:

$$d(t)^{T}((1+\tau_{s})\Pi_{i,k}-(1+a_{i})(\bar{G}_{i}-\bar{F}_{i,k}C)^{T}\Pi_{i,k}(\bar{G}_{i}-\bar{F}_{i,k}C) -(1+a_{i}^{-1})\theta_{i,k}\bar{\beta}_{i}^{2}\bar{T}_{i}^{T}\bar{T}_{i}-I)d(t) \geq 0$$
(24)

Equation (25) confirms (24).

$$(1+\tau_s)\Pi_{i,k} - (1+a_i)(\bar{G}_i - \bar{F}_{i,k}C)^T\Pi_{i,k}(\bar{G}_i - \bar{F}_{i,k}C) - (1+a_i^{-1})\theta_{i,k}\bar{\beta}_i^2\bar{T}_i^T\bar{T}_i - I \ge 0$$
 (25)

Equation (25) is transformed into equation (26) by using the Schur complement lemma:

$$\begin{pmatrix}
(1+\tau_s)\Pi_{i,k} - (1+a_i^{-1})\theta_{i,k}\bar{\beta}_i^2\bar{T}_i^T\bar{T}_i - I & \sqrt{1+a_i}(\bar{G}_i - \bar{F}_{i,k}C)^T \\
* & \Pi_{i,k}^{-1}
\end{pmatrix} \ge 0$$
(26)

Using $\Pi_{i,k} = \rho V_{i,k}^{-1}$ and $\theta_{i,k} = \Psi_{i,k}^{-1}$, and multiplying inequality (26) by $bdiag(V_{i,k}^{T}, I)$ as well $bdiag(V_{i,k}, I)$, accordingly:

$$\begin{pmatrix}
(1+\tau_{s})V_{i,k} - (1+a_{i}^{-1})\Psi_{i,k}^{-1}\overline{\beta}_{i}^{2}\overline{V}_{i,k}^{T}\overline{T}_{i}^{T}\overline{T}_{i}V_{i,k} - V_{i,k}^{T}IV_{i,k} & \sqrt{1+a_{i}}V_{i,k}^{T}(\overline{G}_{i} - \overline{F}_{i,k}C)^{T} \\
* & V_{i,k}
\end{pmatrix} \ge 0$$
(27)

Using change of variable $O_{i,k} = F_{i,k} CV_{i,k}$ and Schur complement lemma, it gets:

$$\begin{pmatrix}
(1+\tau_{s})V_{i,k} & \sqrt{1+a_{i}^{-1}}\overline{\beta}_{i}V_{i,k}^{T}\overline{T}_{i} & V_{i,k}^{T} & \sqrt{1+a_{i}}(V_{i,k}^{T}\overline{G}_{i}^{T}-O_{i,k}^{T}) \\
* & \Psi_{i,k}I & 0 & 0 \\
* & * & I & 0 \\
* & * & * & V_{i,k}
\end{pmatrix} \ge 0$$
(28)

Equation (20) is expressed as follows:

$$V_{i,k} - \Psi_{i,k} I \ge 0 \tag{29}$$

Hence, equations (28) and (29) validate the first and second constraints stated in (15), correspondingly. Consequently, the second condition of the enhancement issue stated in (14) is expanded as:

$$I_{i}(e(k_{s})) \leq fI_{i}(e(k_{s})) \Rightarrow fd(k_{s})^{T} \Pi_{i}d(k_{s}) - d(t_{s})^{T} \Pi_{i}d(t_{s}) \geq 0$$

$$\Rightarrow d(k_{s})^{T} (f \Pi_{i} - \Pi_{i})d(k_{s}) \geq 0$$
(30)

If equation (30) is true, then equation (29) is true.

$$f \prod_{i} - \prod_{i} \ge 0 \Rightarrow f V_{i}^{-1} - V_{i}^{-1} \ge 0 \Rightarrow V_{i} - f^{-1} V_{i} \ge 0$$
 (31)

Therefore, equation (31) proves the third restriction in equation (15). In the subsequent, the third condition in equation (14) is extended as follows:

Summing the first condition in equation (14) in equation (14) from r = 0 to $r \to \infty$, it has:

$$\sum_{r=0}^{\infty} [d(t+1)^{T} \Pi_{i,k} d(t+1) - d(t)^{T} \Pi_{i,k} d(t)]$$

$$\leq \tau_{s} \sum_{t=0}^{\infty} d(t)^{T} \Pi_{i,k} d(t) - \sum_{t=0}^{\infty} d(t)^{T} d(t)$$
(32)

By considering the objective function in equation (10), it obtains:

$$d(k \mid k)^{T} \Pi_{i,k} d(k \mid k) \leq -J_{\infty} \Rightarrow J_{\infty} \leq d(k \mid k)^{T} \Pi_{i,k} d(k \mid k) \Rightarrow d(k)^{T} \Pi_{i,k} d(k) \leq \rho_{i,k}$$

$$\Rightarrow -1 + d(k)^{T} \rho_{i,k}^{-1} \Pi_{i,k} d(k) \leq 0$$
(33)

Considering $\Pi_{i,k} = \rho V_{i,k}^{-1}$, equation (33) is formed as:

So, equation (34) verifies the fourth constraint in equation (15). Then, the fourth condition in equation (14) is extended as follows:

$$\begin{aligned} \left| d_{m}(t) \right|^{2} &= \left| (\Pi_{i,k}^{-\frac{1}{2}} \Pi_{i,k}^{-\frac{1}{2}} d(t))_{m} \right|^{2} \leq \rho_{i,k} \left| (\Pi_{i,k}^{-\frac{1}{2}})_{m} \right|^{2} = \rho_{i,k} V^{m} \Pi_{i,k}^{-1} V^{mT} \leq d_{m,\max}^{2} \\ \Rightarrow \begin{pmatrix} d_{m,\max}^{2} & V^{m} \\ * & \rho_{i,k}^{-1} \Pi_{i,k} \end{pmatrix} \geq 0 \Rightarrow \begin{pmatrix} d_{m,\max}^{2} & V^{m} \\ * & V_{i,k}^{-1} \end{pmatrix} \geq 0 \Rightarrow \begin{pmatrix} I & 0 \\ 0 & V_{i,k} \end{pmatrix}^{T} \begin{pmatrix} d_{m,\max}^{2} & V^{m} \\ * & V_{i,k}^{-1} \end{pmatrix} \\ \begin{pmatrix} I & 0 \\ 0 & V_{i,k} \end{pmatrix} \geq 0 \Rightarrow \begin{pmatrix} d_{m,\max}^{2} & V^{m} V_{i,k} \\ * & V_{i,k} \end{pmatrix} \geq 0 \end{aligned}$$

$$(35)$$

Equation (35) confirms fifth constraint in equation (15).

In the following, the recursive feasibility is ensured. Summing both sides of equation (16) from j = 0 to j = l, it has:

$$\sum_{r=0}^{l} [d(t+1)^{T} \Lambda_{i,k} d(t+1) - d(t)^{T} \Lambda_{i,k} d(t)]$$

$$\leq \tau_{s} \sum_{r=0}^{l} d(t)^{T} \Pi_{i,k} d(t) - \sum_{r=0}^{l} d(t)^{T} d(t)$$

$$\Rightarrow d(k+r+1|k)^{T} \Pi_{i,k} d(k+r+1|k) - d(k|k)^{T} \Lambda_{i,k} d(k|k) \leq 0$$

$$\Rightarrow d(k+l+1|k)^{T} \Pi_{i,k} d(k+l+1|k) \leq d(k|k)^{T} \Lambda_{i,k} d(k|k)$$

$$\Rightarrow d(k+r+1|k)^{T} \Pi_{i,k} d(k+r+1|k) \leq \rho_{i,k}$$
(36)

Setting 1 = 0, it has:

$$d(k+1|k)^{T} \prod_{i,k} d(k+1|k) \le \rho_{i,k}$$
(37)

On the other hand, equation (33) at sample k + 1 is written as follows:

$$d(k+1|k+1)^{T} \prod_{i,k+1} d(k+1|k+1) \le \rho_{i,k+1}$$
(38)

By analysing equations (37) and (38), it is inferred that $(\rho_{i,k}, \Pi_{i,k})$ can serve as a feasible resolution at the k+1 sample. Consequently, the recursive feasibility is guaranteed. Since $(\rho_{i,k+1}, \Pi_{i,k+1})$ displays an optimal solution at the k+1 sample, it can express:

$$\rho_{i,k+1} \le \rho_{i,k} \Rightarrow d(k+1|k+1)^T \Lambda_{i,k+1} d(k+1|k+1) \le d(k+1|k)^T \Lambda_{i,k} d(k+1|k)
\Rightarrow I_{i,k+1}(k+1) \le I_{i,k}(k+1|k) \le (1+\tau_s) I_{i,k}(k|k) - d(k|k)^T d(k|k)
\Rightarrow I_{i,k+1}(k+1) \le (1+\tau_s) I_{i,k}(k) - d(k)^T d(k)$$
(39)

The switching rule is determined by the interplay between the PDT structure and the conditions specified in equations (11) and (12). Let k_{s_g+1} represent the first switching time step that happens after k_{s_g} , and $k_{s_{g+1}}$ denote the first switching time step that happens in the (q+1)-th window. The value of I in the qth window undergoes changes based on Definition 1 and is calculated utilising equations (30) and (39):

$$\begin{split} &I_{s\left(k_{q+1}\right)}(e\left(k_{s_{q+1}}\right)) \leq fI_{s\left(k_{s_{q+1}}-1\right)}(d(k_{s_{q+1}})) \leq f\left(1+\tau_{s}\right)I_{\sigma\left(k_{s_{q+1}}-1\right)}(d(k_{s_{q+1}}-1)) \\ &\leq \ldots \leq f\left(1+\tau_{s}\right)^{k_{s_{q+1}}-k_{s_{q+1}-1}}I_{\sigma\left(k_{s_{q+1}-1}\right)}(d(k_{s_{q+1}-1})) \\ &\leq \ldots \leq f^{T(k_{s_{q+1}},k_{s_{q+1}})}(1+\tau_{s})^{k_{s_{q+1}}-k_{s_{q+1}}}I_{s\left(k_{s_{q+1}}\right)}(d(k_{s_{q+1}})) \\ &\leq f^{T(k_{s_{q}},k_{s_{q+1}})}(1+\tau_{s})^{k_{s_{q+1}}-k_{s_{q}}}I_{s\left(k_{s_{q}}\right)}(d(k_{s_{q}})) \\ &\leq f^{T(k_{s_{q}},k_{s_{q+1}})}(1+\tau_{s})^{k_{s_{q+1}}-k_{s_{q}}}I_{s\left(k_{s_{q}}\right)}(d(k_{s_{q}})) \\ &\Rightarrow I_{s\left(k_{s_{q+1}}\right)}(d(k_{s_{q+1}})) \leq e^{T(k_{s_{q}},k_{s_{q+1}})\ln f + (k_{s_{q+1}}-k_{s_{q}})\ln(1+\tau_{s})}I_{s\left(k_{s_{q}}\right)}(d(k_{s_{q}})) \\ &\leq e^{(k_{T}\omega+1)\ln f + k_{m}\ln(1+\tau_{s})}I_{s\left(k_{s_{q}}\right)}(d(k_{s_{q}})) \end{split}$$

If $k_{s0} = 0$ and $k_{sg+1} = k$, then, based on (36):

$$I_{s(k)}(d(k)) \le e^{q((k_T\omega + 1)\ln f + k_m \ln(1 + \tau_s))} I_{s(0)}(d(0))$$
(41)

If $(kT\omega + 1)$ ln f + km $ln(1 + \tau_S) < 0$, then I approaches zero. Consequently, the system achieves asymptotic stability.

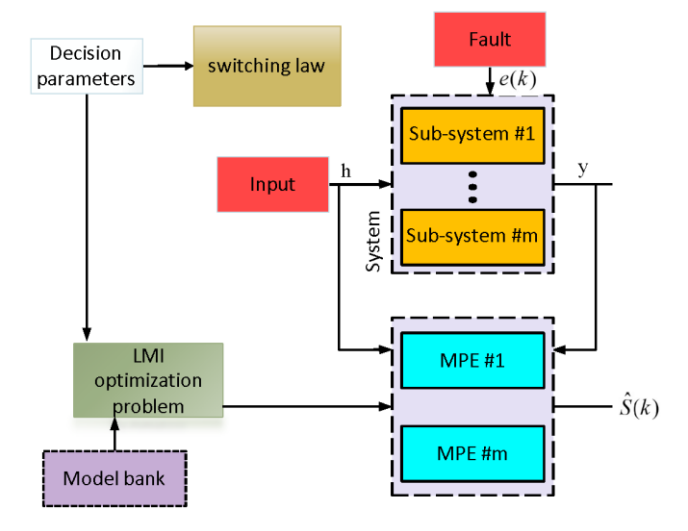
Remark 1: The recommended design is constructed in three sequential stages as outlined below:

Step 1: By considering (τ_S, ε) and (kT,ω) , a set of switching signals is created. These metrics are substituted into (16) to derive the permissible range of the PDT (k_T) .

Step 2: The problem presented in equation (15), according to the current subsystem, is solved at any stage. This process involves determining the estimator gain $(F_{i,k})$ and the matrix $(\Pi_{i,k})$ at any stage while considering the metrics outlined in Stages 1 and 2.

The construction of the estimator is drawn in Figure 1.

Figure 1 The implementation of the recommended estimator (see online version for colours)



4 Numerical simulation

The ongoing stirred tank reactor system is known as the beating heart of the petrochemical industry. In this system, different types of chemical processes are performed. In other words, raw materials with a certain concentration continuously enter the reactor, and these materials are combined and a chemical reaction is carried out at the same time. Finally, the produced product is removed from the reactor. This system is equipped with a thermal jacket that keeps the temperature of the process fixed. Figure 2 shows a sample of a chemical reactor. Here, it is assumed that the following chemical reaction is taking place inside the reactor:

$$P1 \rightleftharpoons P2 \rightarrow P3$$
 (42)

that the species P1 and P2 enter the reactor with the concentrations of C_{P10} and C_{P20} respectively, and the desired product, which is a combination of the desired concentrations C_{P1d} , C_{P2d} and C_{P3d} , leaves the reactor to be If the states and inputs of this chemical reaction are selected as follows:

$$s_1 = \frac{C_{P1}}{C_{P10}}, s_2 = \frac{C_{P2}}{C_{P20}}, s_3 = \frac{C_{P3}}{C_{P10}}, u = \frac{N_{P20}}{R_V C_{P10}}$$
(43)

which R_V displays the volumetric flow rate and N_{P20} displays the molar flow rate of P2, then the chemical kinetic equations will be as follows:

$$\dot{s}_{1} = 1 - s_{1} - Gb_{1}s_{1} + Gb_{2}s_{2}^{2}$$

$$\dot{s}_{2} = Gb_{1}s_{1} - s_{2} - Gb_{2}s_{2}^{2} - Gb_{3}s_{2}^{2} + u$$

$$\dot{s}_{3} = Gb_{3}s_{2}^{2} - s_{3}$$
(44)

where $Gb_i(i=1,2,3)$ present the metrics of the chemical reaction. Let $x_1 \equiv s_1 - s_{1d}$, $x_2 \equiv s_2 - s_{2d}$, $x_3 \equiv s_3 - s_{3d}$, and $h = u - u_d$. By inducing the actuator fault to the system dynamic and discretising the continuous dynamic using Euler strategy based on the metrics given in Table 1, the state-space representations of the modes is written as follows:

Figure 2 Diagram of the continuous stirred tank reactor (CSTR) system (see online version for colours)

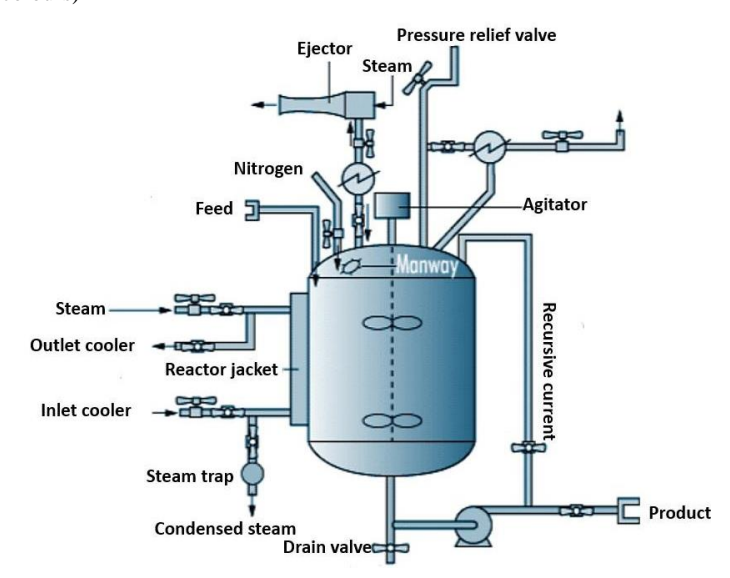


Table 1 The metrics of the CSTR system

| Metrics | Values |
|------------------------------|---|
| Desired states | $x_{d} = [0.34670.87960.8796]^{T}, u_{d} = 1$ |
| metrics of chemical reaction | $mod\ e\ 1:\ Gb_1=\ 3,\ Gb_2=\ 0.5,\ Gb_3=1$ |
| Sampling time | 0.1 s |

Mode 1:

$$\begin{aligned} 0.6 & 0.087 & 0 & 0 & 0 & 0.05x_2^2(k) \\ x\left(k+1\right) &= \begin{pmatrix} 0.3 & 0.637 & 0 \\ 0 & 0.175 & 0.9 & 0 & 0 \end{pmatrix} x\left(k\right) + \begin{pmatrix} 0.1 \end{pmatrix} k\left(k\right) + \begin{pmatrix} -0.15x_2 & 2(k) \\ 0 & 0.1x_2^2(k) \end{pmatrix} \\ y\left(k\right) &= \begin{bmatrix} 0.01 \end{bmatrix} x\left(k\right) \end{aligned}$$

Mode 2:

$$x(k+1) = \begin{bmatrix} 0.65 & 0.087 & 0 \\ | & & & \\ 0.25 & 0.725 & 0 \\ | & 0 & 0.0870 & 0.9 \end{bmatrix} x(k) + \begin{bmatrix} 0 \\ | & \\ 0.1 \\ | & \\ 0 \end{bmatrix} h(k) + \begin{bmatrix} 0 \\ | & \\ 0.1 \\ | & \\ 0 \end{bmatrix} e(k) + \begin{bmatrix} 0.05x^{2}(k) \\ | & \\ -0.1x^{2}(k) \\ | & \\ 0.05x^{2}(k) \\ | & \\ 0 \end{bmatrix}$$

$$y(k) = \begin{bmatrix} 0 & 0 & 1 \end{bmatrix} x(k)$$

Considering that it is not possible to measure all chemical reaction concentrations, an observer should be used to solve this challenge. Also, due to the possibility of an actuator fault occurring in this system, the observer must be developed into a fault estimator that can both detect the fault occurrence time and measure its exact value. This is the first step to form a regulator based on the fault estimator, so that despite the existence of the fault, the concentrations can be brought to their desired value and a high-quality product can be produced in the shortest time. Based on this, the estimator designed in this paper is recommended. According to the process of changing the concentration of input raw materials, which leads to changing the dynamics of the chemical reaction, the characteristics of the switching signal are determined. These specifications are provided in Table 2. This specification refers to a set of switching signals that are allowed to be applied to the system. If the switching signal outside this set is applied to the system, the optimal performance of the estimator or even its stability will be jeopardised. Therefore, to determine these specifications, an expert familiar with the system should be consulted. In the following, the relation (16) is used to calculate k_m According to this relationship, the value of k_m will be equal to 4.5 step.

Now, to simulate the estimator on the system, a switching signal is selected as a member of the set $S_{PDT}(\omega = 0.1 \frac{1}{step}, k_T = 10 \text{ step}, k_m = 4.5 \text{ step})$ as shown in Figure 3. It

should be noted that the concept of PDT helps to make this class bigger so that it is easier to think about the possibility of the estimator becoming unstable.

 Table 2
 Design metrics

| Metrics | Values |
|-----------------------------|--|
| PDT specifications | $\tau s = -0.1, f = 1.1, kT = 10step, \omega = 0.4 \frac{1}{step}$ |
| Nonlinear metrics | $a = a2 = 1$, $\beta 1 = 0.15$, $\beta 2 = 0.1$, $T1 = T2 = I$ |
| Estimation error saturation | $ di \le 1i = 1,2,3$ |

In the following, the simulation is carried out through two scenarios, and the outcomes are analysed.

Scenario 1: No actuator fault (e(k) = 0)

By simulating the chemical system and the recommended estimator, the peak of the efficiency metric converges to zero, as shown in Figure 4. This figure confirms that the peak of the efficiency metric is strictly downward, and at each time step it guarantees that the answer exists for future time steps. Therefore, the recommended estimator continues to work without stopping and overcomes the feasibility challenges in the real world, and consequently, the reliability of the regulation network rises. The energy function of the network is also plotted in Figure 5. According to the Lyapunov criterion, if the changes in the energy function are negative, or in other words, the value of the energy function reaches zero, asymptotic stability is confirmed. Therefore, the recommended scheme shows a coordination between the estimator and the shifting signal, which leads to the asymptotic equilibrium of the system. Figure 6 also shows the obtained state estimation error, which has satisfactory behaviour and approaches zero at the right time. Also, the error rate does not exceed a specified saturation bound.

Figure 3 Shifting signal (see online version for colours)

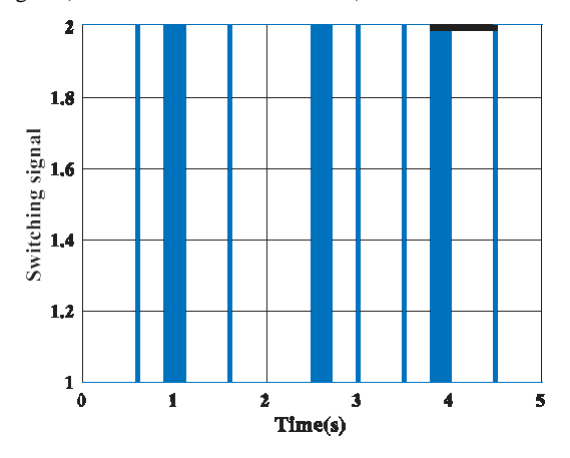


Figure 4 Upper limit of the efficiency metric (see online version for colours)

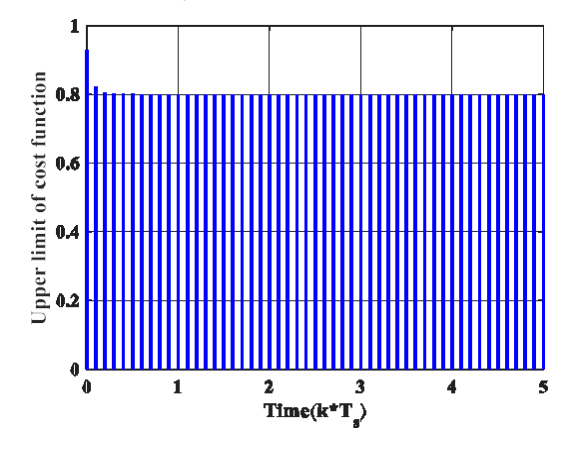


Figure 5 Energy function (see online version for colours)

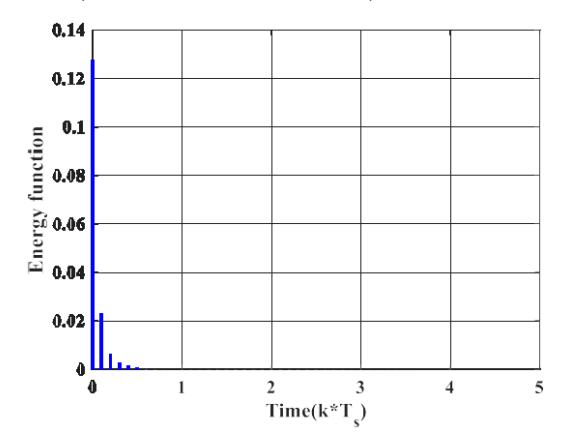


Figure 6 State estimation error (see online version for colours)

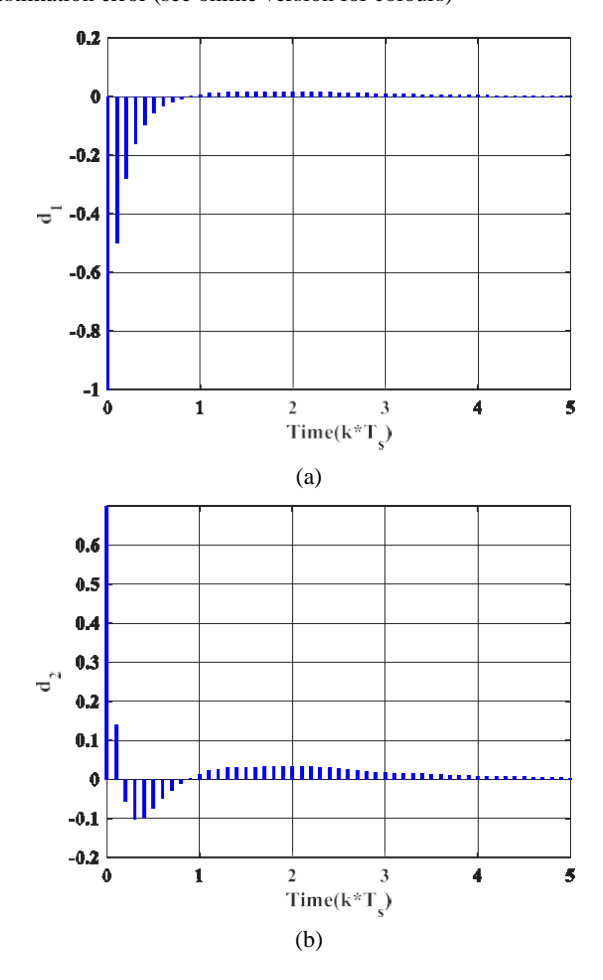
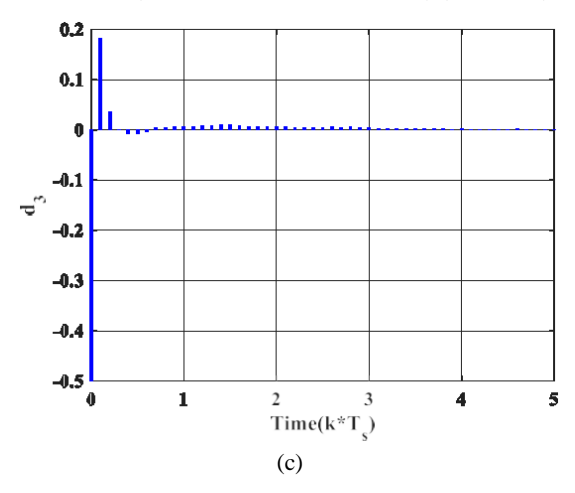
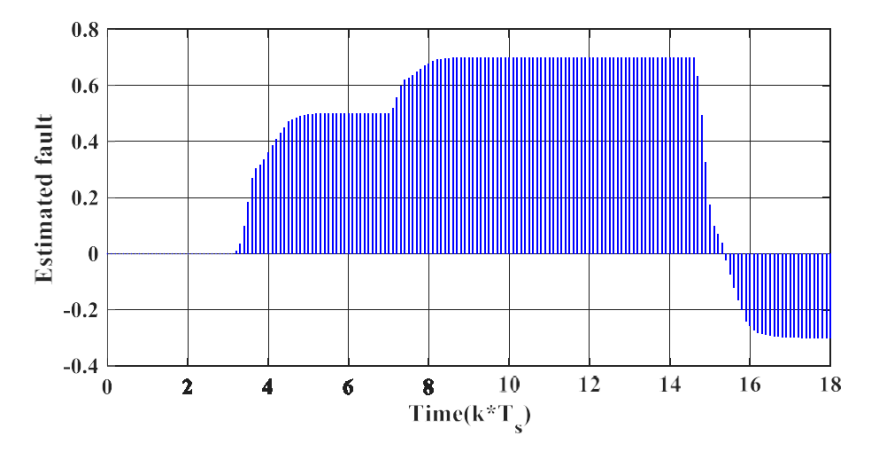


Figure 6 State estimation error (see online version for colours) (continued)



Scenario 2: Here, the performance of the estimator is evaluated against different faults that occur at different times. In the design of the estimator, it was assumed that the fault changes are constant. Therefore, it is expected that the recommended estimator will perform satisfactorily against constant faults, exponential faults with small changes, and constant slope faults. This issue is depicted in Figures 7 and 8. It should be noted that for the estimator to be able to estimate a larger class of faults, the augmented system must be formed with higher derivatives of the faults so that it can follow the behaviour of these faults well.

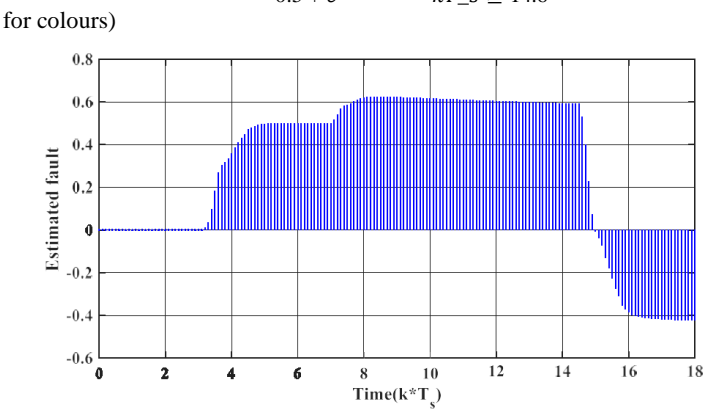
Figure 7 Fault estimation $(e(k)) = \begin{cases} 0.53.1 \le kT_.s < 7 \\ 0.77 \le kT_.s < 14.6 \\ -0.3kT_.s \ge 14.6 \end{cases}$ (see online version for colours)



$$0kT_s < 3.1$$

 $0.53.1 \le kT_s < 7$

Figure 8 Fault estimation ($e(k) = 0.5 + e^{-0.01(kT-s^{-7})}$ 7 $\leq kT_s < 14.6$ (see online version $-0.5 + e^{-0.01(kT-s^{-7})}kT$ $s \geq 14.6$



5 Discussion

The simulation findings from the continuous stirred tank reactor system confirm the efficacy and resilience of the proposed model predictive fault estimation methodology under both nominal and defective operating circumstances. In the absence of actuator defects, the performance metric defined as the squared Euclidean norm of the state estimation error throughout the prediction horizon demonstrated a tight monotonic decline, converging to zero within 20 sampling intervals. This behaviour validates the estimator's stability and the legitimacy of the recursive feasibility and asymptotic stability assurances derived from the Lyapunov-based analysis and the linear matrix inequality framework. The state estimation error constantly stayed within the defined saturation limit, illustrating the method's reliability and accuracy. In fault situations characterised by continuous, exponentially variable, and linearly increasing disturbances, the estimator precisely identified the initiation and amplitude of the faults. The stability of the estimation error dynamics was maintained, as demonstrated by the ongoing reduction in the Lyapunov-based energy function. These results underscore the estimator's ability to adjust to various fault patterns while preserving resilience amid fluctuating system dynamics. This performance was attained without the necessity of explicitly modelling fault dynamics beyond first-order behaviour, highlighting the usefulness of the suggested method.

Compared to traditional fault diagnostic methods, such as Leuenberger observers and UIOs which frequently overlook the influence of fault dynamics or depend on stringent assumptions on system switching behaviour the suggested estimator provides a more universal and adaptable framework. By integrating a continuous dwell-time switching mechanism and developing an enhanced state-space representation that incorporates fault factors, the estimator proficiently manages systems functioning across various regimes. The incorporation of a saturation restriction on the estimation error improves robustness against modelling mistakes and noise, reducing the likelihood of false alarms or

instability in real-world scenarios. The proposed method offers a notable advantage in computing efficiency. The bifurcation of the estimator design into offline and online phases guarantees minimal real-time computational requirements. In the offline phase, parity vectors and predictive structures are developed using previous input-output data from various operating modes. The online phase necessitates only residual generation and constraint evaluation, rendering the estimator appropriate for real-time industrial applications, especially in resource-limited embedded systems. Notwithstanding its advantages, the suggested framework possesses specific limits that necessitate additional examination. The existing formulation presumes that fault signals develop gradually or remain stable over time.

As a result, the estimator may demonstrate diminished accuracy in situations characterised by sudden or higher-order fault dynamics. Future research should aim to expand the enhanced state-space model to include higher-order fault derivatives, so facilitating more precise monitoring of intricate fault dynamics. Furthermore, although the continuous stirred tank reactor exemplifies a case study in chemical process systems, extensive validation across various nonlinear switched systems such as power electronics, autonomous vehicles, or cyber-physical systems is essential to establish the method's general applicability. A crucial focus entails the systematic assessment of the estimator's robustness amongst model uncertainty, external disturbances, and sensor noise, which are frequently encountered in industrial settings. Future study may investigate the incorporation of multi-objective control strategies into the estimate framework, including the amalgamation of energy minimisation goals with worst-case disturbance rejection standards. Such enhancements would augment performance in demanding operational settings. The shift of the suggested estimator from simulation to experimental validation via hardware-in-the-loop testing or implementation on pilot-scale industrial systems constitutes a crucial step towards real-world application and technological adoption.

This research offers a practical contribution through its possible application in real-time monitoring and fault-tolerant control systems for safety-critical industrial processes, especially in chemical manufacturing settings. The proposed estimator, through effective use in a continuous stirred tank reactor system, can be utilised to monitor actuator integrity and identify faults at early stages, facilitating prompt intervention before system deterioration or failure. The offline online computational architecture renders it appropriate for embedded control platforms with constrained processing capabilities, facilitating efficient deployment in programmable logic controllers or industrial automation systems. Moreover, the estimator's capacity to precisely ascertain fault magnitude and uphold stability throughout switching dynamics enables it to function as a fundamental component in the creation of a robust fault-tolerant regulator. This may result in increased system reliability, less downtime, and superior product quality across diverse operational contexts.

6 Conclusion

This paper introduced a defect estimation methodology utilising a model predictive technique for switched nonlinear systems. The process initiates with the development of an enhanced state-space model that integrates system states and fault factors. The squared Euclidean norm of the estimate error throughout the prediction horizon was established as the performance metric. The challenge of minimising this metric was restated using

model predictive control principles and stability requirements as the minimisation of its upper limit, subject to linear matrix inequality criteria that guarantee the asymptotic stability of the estimation error dynamics. A saturation constraint was applied to the estimation error to provide constrained performance, hence enhancing robustness against shocks and modelling uncertainties. The theoretical assurance of recursive feasibility for the proposed estimator was tested at each time step, ensuring consistent real-time functioning. The estimator was evaluated on a continuous stirred tank reactor system, a standard in the petrochemical sector, and the findings validated its precision in fault detection and estimating under both normal and defective settings.

Notwithstanding its benefits, the suggested method presupposes slowly shifting or continuous fault dynamics, thereby constraining its efficacy in situations characterised by sudden or high-frequency faults. Moreover, the existing implementation is limited to validation through simulation. The framework can be expanded to include higher-order fault dynamics and accommodate systems with greater model uncertainty and noise. The incorporation of multi-objective optimisation, encompassing both energy-based (H_2) and worst-case disturbance ($H\infty$) criteria, may augment its robustness. Furthermore, experimental validation on physical systems or integrated industrial platforms is a crucial step towards real-world implementation and practical utilisation.

Acknowledgement

This work was supported by the Science and Technology Research Program of Chongqing Municipal Education Commission (Grant No.KJZD-K202203202).

Conflicts of interest

All authors declare that they have no conflicts of interest.

References

- Abbasi, M.A. and Huang, S. (2024) 'Development of a fault diagnostics and tolerance system: an application to continuous stirred tank reactor', *Measurement Science and Technology*, Vol. 35, No. 6, p.066203.
- Chen, H., Du, D., Zhu, D. and Yang, Y. (2019) 'UIO-based fault estimation and accommodation for nonlinear switched systems', *International Journal of Control, Automation and Systems*, Vol. 17, No. 2, pp.435–444.
- Du, D., Cocquempot, V. and Jiang, B. (2019) 'Robust fault estimation observer design for switched systems with unknown input', *Applied Mathematics and Computation*, Vol. 348, pp.70–83.
- Duník, J., Straka, O., Kost, O., Tang, S., Imbiriba, T. and Closas, P. (2024) 'Noise identification for data-augmented physics-based state-space models', 2024 IEEE Workshop on Signal Processing Systems (SiPS), USA pp.101–106.
- Geromel, J.C. (2023) 'Differential linear matrix inequalities', *Differential Linear Matrix Inequalities: In Sampled-Data Systems Filtering and Control*, Springer, Switzerland, pp.19–35.

- Granzotto, M., De Silva, O.L., Postoyan, R., Nešić, D. and Jiang, Z-P. (2024) 'Robust stability and near-optimality for policy iteration: for want of recursive feasibility, all is not lost', *IEEE Transactions on Automatic Control*, Vol. 69, No. 12, 20 May, pp.8247–8262.
- Li, Y. and Tong, S. (2017) 'Adaptive neural networks prescribed performance control design for switched interconnected uncertain nonlinear systems', *IEEE Transactions on Neural Networks and Learning Systems*, Vol. 29, No. 7, pp.3059–3068.
- Li, Y., Tong, S., Liu, L. and Feng, G. (2017) 'Adaptive output-feedback control design with prescribed performance for switched nonlinear systems', *Automatica*, Vol. 80, pp.225–231.
- Liu, J., Yang, J., Yan, Y., Tan, Y., Wang, X. and Li, S. (2024) 'On recursive feasibility and stability of constrained output regulation', *IEEE Transactions on Automatic Control*.
- Liu, Q. and Zhao, J. (2020) 'Switched adaptive observers design for a class of switched uncertain nonlinear systems', *Nonlinear Analysis: Hybrid Systems*, Vol. 36, p.100866.
- Lyu, X., Ai, Q., Yan, Z., He, S., Luan, X. and Liu, F. (2020) 'Finite-time asynchronous resilient observer design of a class of non-linear switched systems with time-delays and uncertainties', *IET Control Theory and Applications*, Vol. 14, No. 7, pp.952–963.
- Nodozi, I. and Rahmani, M. (2017) 'LMI-based model predictive control for switched nonlinear systems', *Journal of Process Control*, Vol. 59, pp.49–58.
- Petersen, I.R. (1987) 'A stabilization algorithm for a class of uncertain linear systems', *Systems and Control Letters*, Vol. 8, No. 4, pp.351–357.
- Qi, Y., Yu, W., Huang, J. and Yu, Y. (2021) 'Model predictive control for switched systems with a novel mixed time/event-triggering mechanism', *Nonlinear Analysis: Hybrid Systems*, Vol. 42, p.101081.
- Sarbaz, M. (2024) 'Model predictive control for interval type-2 fuzzy systems with unknown timevarying delay in states and input vector', *International Journal of Uncertainty*, *Fuzziness and Knowledge-Based Systems*, Vol. 32, No. 3, pp.385–401.
- Shi, S., Shi, Z. and Fei, Z. (2019) 'Asynchronous control for switched systems by using persistent dwell time modeling', *Systems and Control Letters*, Vol. 133, p.104523.
- Taghieh, A. and Shafiei, M.H. (2021) 'Observer-based robust model predictive control of switched nonlinear systems with time delay and parametric uncertainties', *Journal of Vibration and Control*, Vol. 27, Nos. 17–18, pp.1939–1955.
- Wang, Q., Hu, H. and Zhou, Y. (2024) Memorymamba: Memory-Augmented State Space Model for Defect Recognition, ArXiv Preprint ArXiv: 2405.03673.
- Zhang, J., Zhang, R., Zhou, Y., Li, X. and Zhao, J. (2024) 'A novel model predictive observer for switched systems using dissipativity theory', *Multiscale and Multidisciplinary Modeling*, *Experiments and Design*, pp.1–15.
- Zhang, L., Zhuang, S. and Shi, P. (2015) 'Non-weighted quasi-time-dependent H∞ filtering for switched linear systems with persistent dwell-time', *Automatica*, Vol. 54, pp.201–209.
- Zhang, S., Jia, R., Cao, Y., He, D. and Yu, F. (2024) 'Stable predictive control of continuous stirred-tank reactors using deep learning', *Information Sciences*, Vol. 678, p.120970.
- Zheng, H., Sun, G., Ren, Y. and Tian, C. (2018) 'Quasi-time-dependent controller for discrete-time switched linear systems with mode-dependent average dwell-time', *Asian Journal of Control*, Vol. 20, No. 1, pp.263–275.
- Zheng, Q., Xu, S. and Zhang, Z. (2020) 'Nonfragile H∞ observer design for uncertain nonlinear switched systems with quantization', *Applied Mathematics and Computation*, Vol. 386, p.125435.
- Zuo, S., Liu, X., Jiao, J., Charles, D., Manavoglu, E., Zhao, T. and Gao, J. (2022) Efficient Long Sequence Modeling Via State Space Augmented Transformer, ArXiv Preprint ArXiv: 2212.08136.

Nomenclature

| Abbrevi | iations |
|-------------------------------|--|
| ADT | Average Dwell Time |
| PDT | Persistent Dwell Time |
| MLF | Multiple Lyapunov Functions |
| UIO | Unknown Input Observer |
| MPC | Model Predictive Control |
| DLMI | Discrete-time Linear Matrix Inequality |
| CSTR | Continuous Stirred Tank Reactor |
| PI | Policy Iteration |
| Symbol | |
| e | Faults |
| С | The state-space matrices |
| $G_{s(k)}$ | The state-space matrices |
| $H_{s(k)}$ | The state-space matrices |
| f | The energy variation |
| h | Inputs |
| I | The energy function |
| $J_{s(k)}$ | The state-space matrices |
| k_s | The switching time step |
| N_{P20} | The molar flow rate |
| R_V | The volumetric flow rate |
| s(k) | The switching signal |
| \mathcal{S} | The state estimation |
| x | The states |
| \hat{y} | The output estimation |
| y | Outputs |
| Greek s | ymbol |
| $\overline{\eta_{\sigma(k)}}$ | The nonlinear term |
| $ ho_{i,k}$ | The maximum of the objective metric |